



Contents lists available at ScienceDirect

Computers and Chemical Engineering

journal homepage: www.elsevier.com/locate/compchemeng



A systematic simulation-based process intensification method for shale gas processing and NGLs recovery process systems under uncertain feedstock compositions

Jian Gong, Minbo Yang, Fengqi You*

Robert Frederick Smith School of Chemical and Biomolecular Engineering, Cornell University, Ithaca, New York 14853, USA

ARTICLE INFO

Article history:

Received 18 August 2016

Received in revised form 5 November 2016

Accepted 10 November 2016

Available online xxx

Keywords:

Shale gas processing

NGLs recovery

Feedstock uncertainty

Process intensification

Techno-economic analysis

ABSTRACT

Handling uncertainty in feedstock compositions is an important challenge for shale gas processing and natural gas liquids (NGL) recovery process systems. If the process system is designed without considering uncertain feedstock compositions, the product specifications could be easily violated. To address this challenge, we develop a systematic simulation-based process intensification method. This method consists of three steps, namely process simulation, capacity-oriented process intensification, and design validation. An iterative feature of the proposed method guarantees the intensified design hedged against uncertain feedstock compositions. The proposed method is illustrated on a conventional process system and a novel condensation-based system. In the novel system, a condensation process is considered in the gas dehydration section and it is integrated with a turboexpander process to improve the overall energy utilization efficiency. The intensified design of the novel system shows a lower total annualized cost than that of the conventional system.

© 2016 Elsevier Ltd. All rights reserved.

1. Introduction

Process intensification, as a general goal of process development and design, aims at substantially improving process performance with a wide spectrum of chemical engineering skills (Moulijn et al., 2008). Compared with the original process, an intensified process could retain its primary process objectives, while improving one or more performance parameters which could include economics, environmental impacts, physical plant size, employment, flexibility, controllability, robustness, reliability, safety, etc. (Ponce-Ortega et al., 2012; Lutze et al., 2010, 2013, 2012; Errico et al., 2008; Freund and Sundmacher, 2008). One important area, where process intensification can play a crucial role, is to handle uncertainty. A process system is typically designed using deterministic input parameters, while uncertainty can inevitably undermine the expected performance. An intensified process system, in contrast, considers varying input parameters and results in a much more reliable set of design and operations decisions in order to tackle uncertainty. Therefore, a major goal of this work is to develop a systematic process intensification framework for hedging against uncertainties.

In recent years, shale gas is regarded as an important driver leading the changes in North America's energy landscape (Kerr, 2010; Siirila, 2014). Due to the successful application of advanced extraction technologies, total natural gas production in the U.S. is predicted to increase by 45% by 2040 (EIA, 2015). As a result of the boom in upstream shale gas production, there is a need for additional facilities to absorb the burgeoning supplies of shale gas (Goellner, 2012). Shale gas processing systems remove valuable natural gas liquids (NGL) and undesired constituents from raw shale gas (Speight, 2013) and serve as important components in the shale gas value chain (Gao and You, 2015a). The rapid expansion of the shale gas industry will expedite the deployment of more shale gas processing systems in the near future. An important issue complicating the design of novel shale gas processing systems, however, involves handling uncertainty in feedstock compositions (Liu et al., 2011). Shale gas from various shale plays is subject to significantly different compositions and processing needs (Bullin and Krouskop, 2009). Even for a given shale play, the gas production rate could change throughout the lifetime of each well. Since a shale gas processing plant is usually designed to process raw shale gas collected from multiple shale wells (Reed, 2013; Johnson, 2009; He and You, 2016), the composition of the received feedstock usually keeps fluctuating. If a processing plant is designed to process shale gas with fixed compositions, a large amount of off-spec gas will be produced when the real composition deviates from the designed composi-

* Corresponding author.

E-mail address: fengqi.you@cornell.edu (F. You).

tion. In order to maintain stable supply of qualified gas products, uncertain feedstock compositions must be considered in the intensified shale gas processing system.

In this work, we develop a systematic simulation-based process intensification method for shale gas processing and NGLs recovery process systems under uncertain feedstock compositions. A deterministic design upgrades raw shale gas with a fixed feedstock composition, while a corresponding intensified design in this work applies the same process layout, but employs equipment units with strengthened capacities to hedge against uncertain feedstock compositions. In order to build an intensified design, we first perform detailed process modeling and rigorous process simulation for a set of deterministic designs. Next, the capacity of each unit in the intensified design is selected as the highest operating level of the same unit in the deterministic designs. As an integral part of the intensified design, the operating conditions when feedstock uncertainty is realized are estimated as the set of deterministic operating conditions resulting in the highest operating cost. For the purpose of comparison, a thorough techno-economic analysis is later conducted for the deterministic designs and the intensified design. Lastly, we test all the designs with representative compositions and the entire procedure is iterated until there is no more feasibility issues in the intensified design. We consider two shale gas processing and NGLs recovery process systems for illustration of the proposed method. A novel process system consists of a monoethanolamine (MEA) absorption process in an acid gas removal (AGR) section, a condensation process in a gas dehydration section, a turboexpander process in an NGLs recovery section, and a triethylene glycol (TEG) absorption process in an NGLs dehydration section. The condensation process and the turboexpander process are further integrated to improve the overall energy utilization efficiency. The systems are used to process raw shale gas from 8 wellsites and generate pipeline gas for a downstream power plant. The results are compared between the deterministic designs and the intensified designs, as well as between the two process systems.

The novelties of the work are summarized as follows:

- A systematic simulation-based process intensification method for shale gas processing and NGLs recovery process systems under uncertain feedstock compositions;
- A novel condensation-based process design for shale gas processing and NGLs recovery processes.

The rest of the paper is organized as follows. A literature review for recent studies on the design and synthesis of shale gas processing systems is presented in Section 2. Section 3 presents the simulation-based process intensification method. In Section 4, we describe process details of a novel shale gas processing system and a conventional shale gas processing system. We analyze the economic performance of the deterministic and intensified designs in Section 5. The conclusion is given in Section 6.

2. Literature review

Several publications address the design and synthesis of shale gas processing and/or chemical production from shale gas. El-Halwagi and co-workers developed a process for the production of methanol from shale gas (Ehlinger et al., 2014). In a later contribution, researchers from the same group extended the results by considering four reforming options and evaluating the sustainability performance of the improved processes (Julian-Duran et al., 2014). A techno-economic analysis was performed for a polygeneration process with methane oxidative coupling based on shale gas feedstock (Salkuyeh and Adams, 2015). Three novel processes

were developed for integrating shale gas processing with ethylene production, and the co-processing of shale gas and ethane cracking gas could significantly increase the profitability of the proposed processes (He and You, 2014). Later, an integrated bioethanol dehydration and methane oxidative coupling process was shown to improve the sustainability of the shale gas processing process (He and You, 2015). These studies focus on feasibility analysis and employ process simulation as the primary tool to establish a feasible process design. Others employ systematic approaches to obtain the optimal designs of shale gas energy systems and supply chains. Water management network systems in shale gas production (Lira-Barragan et al., 2016; Gao and You, 2015c; Yang et al., 2014) and shale gas supply chains (Gao and You, 2015a, 2015b) were optimized with various objective functions.

There are limited contributions addressing feedstock uncertainty in NGLs recovery processes. Getu et al. conducted a thorough techno-economic analysis of six NGLs recovery configurations under eight different feedstock compositions, and concluded that an IPSI-1 scheme offered the best economic performance (Getu et al., 2013). The uncertain feedstock compositions in this work were addressed through a scenario-based analysis, but the obtained designs were not validated further to process other feedstocks. Wang and Xu studied the optimal design and synthesis of integrated NGLs recovery and LNG re-gasification under uncertain feed rates (Wang and Xu, 2014). They assumed a standard normal distribution for uncertain feed rates, and the objective function of the proposed optimization model was to minimize the expected total cost of utilities. Consequently, the resulting optimal process design was not expected to handle the feedstocks in all the scenarios. Since a processing plant operates continuously, off-spec products will be generated if the real feedstock is significantly different from the expected optimal value through the stochastic programming approach. In both contributions, the feedstocks were assumed to contain little or no acid gases and water, so no integration was explored between the NGLs recovery process and upstream purification processes.

Gas processing technologies are commonly employed independent of each other in conventional shale gas processing and NGLs recovery process systems. However, since both condensation-based gas dehydration processes and NGLs recovery processes require a substantial amount of refrigeration, there is a potential opportunity to reduce the total energy consumption through technology integration. To the best of our knowledge, there is no investigation into the technology integration in shale gas processing and NGLs recovery processes. Moreover, existing literature do not report any approach to addressing uncertain feedstock compositions simultaneously in the design and synthesis of shale gas processing and NGLs recovery processes.

Given uncertain feedstock compositions, an intensified process design is desired in order to produce qualified pipeline-quality gas products under changing feedstock conditions. However, a series of research challenges remain unanswered. These challenges include how to identify and generate deterministic process designs, how to develop intensified process designs based on deterministic process designs, and how to validate the product quality of the intensified process designs. Therefore, the goal of this work is to address these research challenges and develop a systematic method to obtain the intensified designs of a novel condensation-based and a conventional shale gas processing and NGLs recovery process systems.

3. Systematic simulation-based process intensification method

In a deterministic process design problem, decisions are made "once and for all". With full knowledge of the feedstock information,

the operating level of each unit does not change over time and thus the minimum capacity of each unit is equal to the fixed operating level. In fact, the feedstock compositions of a shale gas processing facility may vary significantly over time. We can calculate the fraction of component i (such as methane) in the raw shale gas received

$$\sum_i c_{i,j}^{\text{well}} v_j$$

by a processing facility using $\frac{j}{\sum_j v_j}$, where $c_{i,j}^{\text{well}}$ is the fraction

of component i from wellsite j and v_j is the flowrate of wellsite j . The production rate of a shale well is found to gradually decline over time (Zavala-Araiza et al., 2015). In addition, more wells can be completed in the same wellsite to increase the production rate. Therefore, the flowrate v_j rarely remains a fixed level in practice and fluctuation in flowrates can cause significant changes in the feed composition. In this work, we assume the composition of each wellsite is relatively stable (Freeman et al., 2012), and the feedstock composition uncertainty is caused by unstable flowrates of the raw shale gas from different wellsites. In the cases that wellsite compositions also change, the compositions with the highest fractions of undesired materials or NGLs can be easily identified according to the trend of change in the compositions. In the proposed process intensification approach, we use those compositions to construct the deterministic designs.

Due to the uncertain nature in shale gas feedstock compositions, the deterministic designs that show excellent process structure and integration strategies can unfortunately generate off-spec products (Gong and You, 2015). From a practical point of view, we aim for an intensified process design that keeps the process layout of the corresponding deterministic designs, but can be hedged against uncertainty in feedstock compositions. In such intensified designs, equipment capacities are understandably larger than the operating levels for processing a given deterministic feedstock. The key challenge is how to determine the appropriate capacities from infinitely many possible deterministic feedstock compositions.

Ideally, the capacity of an equipment unit in the intensified design should be larger than the operating level of the same unit in any possible deterministic design with the same process layout. In order to obtain the ideal solution, we need to model the operating level of each equipment unit as a complicated multivariate nonlinear function. Unsurprisingly, the function must involve not only the feedstock composition, but also the operating conditions of other units that influence the immediate streams entering the target unit. Yet, the explicit forms of such complicated functions are not available and have not been reported in literature.

Alternatively, we can reformulate the original formula as $\sum_j c_{i,j}^{\text{well}} w_j$, where $w_j = \frac{v_j}{\sum_j v_j}$. Consequently, the feed composition

is a convex combination of the wellsite compositions with varying weights. Therefore, the wellsite compositions represent extreme feedstock conditions and should be given more attention than the ones derived from the wellsite compositions. In this work, we consider the wellsite compositions to develop deterministic designs and determine the capacity of each equipment unit in the intensified design based on the information of the deterministic designs.

The proposed simulation-based process intensification method for shale gas processing and NGLs recovery process system is shown in Fig. 1. The method consists of three steps. The first step is process simulation. Given a set of wellsite compositions, we develop the same number of deterministic designs with each one corresponding to a wellsite composition. The rigorous process simulations are performed in Aspen HYSYS (AspenTech, 2010a). The energy integration is performed in Aspen Energy Analyser (AspenTech, 2010b), and we obtain the energy consumption and generation rates, as

well as equipment capital costs of all utility units. The direct equipment costs of other operation units are evaluated using Aspen Process Economic Analyser (AspenTech, 2010c). The results provide rich process information for establishing an intensified design.

The second step is capacity-oriented process intensification. As mentioned previously, the intensified process design contains the same process layout, but strengthened equipment capacity to hedge against uncertain feedstock compositions. However, equipment capacities alone are not sufficient to determine complete operating conditions, which are critical to fully describe a process design. Therefore, in this step, two essential components of an intensified process design are determined based on the deterministic designs:

- One component is equipment capacity. The capacity of each equipment unit in the intensified design is selected as the largest value among the operating levels of the same unit in the deterministic process designs. Consequently, the equipment capital cost of each unit in the intensified design corresponds to the largest one in all deterministic designs. Note that the selected highest operating levels in fact represent the smallest possible capacities to accommodate all operating levels of the deterministic designs.
- The other component is process operating conditions. Even though a process can handle feedstocks with uncertain compositions, the specific operating conditions should still vary according to the realized feedstock composition. In the proposed method, we consider a conservative estimation of the operating conditions as the set of operating conditions among the deterministic process designs resulting in the largest operating cost. Note that, unlike the equipment unit-level selection of equipment capacities, the operating conditions of all units are selected simultaneously at the system level (Shi and You, 2016; Yue and You, 2016; Gong et al., 2016; Gong and You, 2016). An example of how to select the two components of an intensified design is shown in Fig. 2.

Next, we conduct a techno-economic analysis for the intensified design. We first calculate the annualized capital cost (ACC) as $TDC \cdot \frac{CEPCI_{2015}}{1 + ICC \cdot \frac{CEPCI_{2009}}{CEPCI_{2015}}} \cdot \frac{R \cdot 1+R^{LS-1}}{1+R^{LS-1}}$. In this formula, the total direct cost (TDC) is first multiplied by the sum of 1 and the indirect cost coefficient (ICC) to account for all investment costs. Next, the 2009-dollar value from the economic evaluation software is converted to the 2015-dollar value using chemical engineering plant cost indices ($CEPCI$) (Lozowski, 2015). Last, the total investment is annualized based on interest rate (R) and plant life span (LS). We then calculate the annual operating cost (AOC) as the sum of the feedstock cost (FSC) and the utility cost (UC). Each feedstock or utility cost is determined as the quantity consumed in a year multiplied by the corresponding price. Finally, the total annualized cost (TAC) sums up the ACC and the AOC.

In the last step, or design validation, we test the deterministic and intensified designs with a series of randomly generated feedstock compositions. If all the pipeline gas products satisfy the specifications, the intensified design passes the validation, and the algorithm terminates; otherwise, we add the compositions that cause feasibility problems into the set of wellsite compositions and the algorithm is repeated from the first step.

It is noted that the proposed approach can also be interpreted more specifically as a robust approach within the much broader context of process intensification.

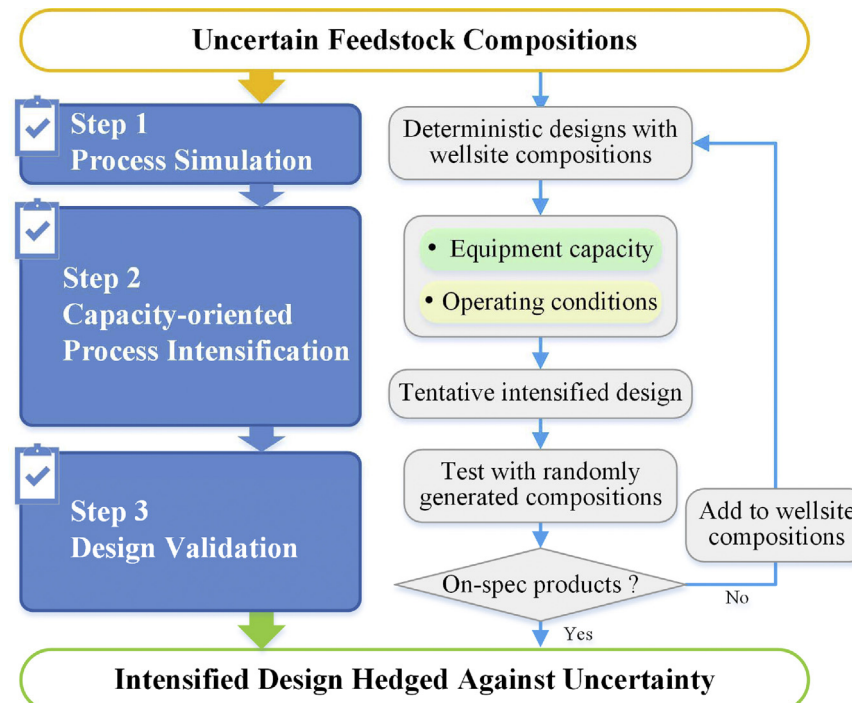


Fig. 1. Flowchart of the proposed simulation-based process intensification method.

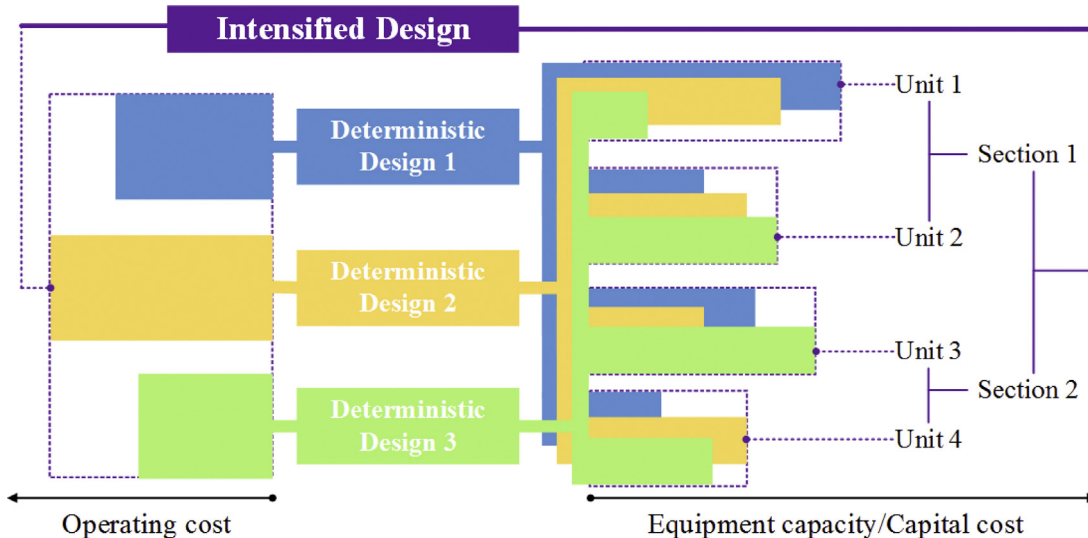


Fig. 2. An example of determining the components of an intensified design of a process with 2 sections and 4 units. The equipment capacities of units 1–4 in the intensified design are selected as the operating levels of the corresponding units from deterministic designs 1, 3, 3, and 2, respectively. The operating conditions in the intensified design are selected as those in deterministic design 2.

4. Process systems description

A shale gas processing and NGLs recovery process is designed to separate most of the valuable NGLs and undesired constituents, so that the resulting gas product meets the specifications for pipeline gas. Depending on the feedstock conditions, shale gas processing can consist of many sections, such as AGR, dehydration, NGLs recovery, nitrogen rejection, etc. In this work, we concentrate on AGR, dehydration, and NGLs recovery as they are the essential sections in most shale gas processing plants. The flowsheet and the description of a nitrogen rejection process are given in the [Appendix A](#). Technologies and processes for other possible sections can be found in the literature ([Kidnay et al., 2011a](#)).

As shown in [Fig. 3](#), two process systems for shale gas processing and NGLs recovery processes are exhibited. In a conventional system ([He and You, 2014](#)), raw shale gas is first purified by MEA absorption to reduce the acid gas components. Next, the water content in the resulting sweet gas is removed by TEG adsorption. Finally, the dry gas is sent to a standalone NGLs recovery process and split into a pipeline product and an NGLs product. In the proposed system, an integrated process for gas dehydration and NGLs recovery simultaneously is considered. To meet the NGLs product specifications, wet NGLs are subsequently sent to a TEG absorption process for dehydration. Details on each technology/process alternative are described in the following subsections.

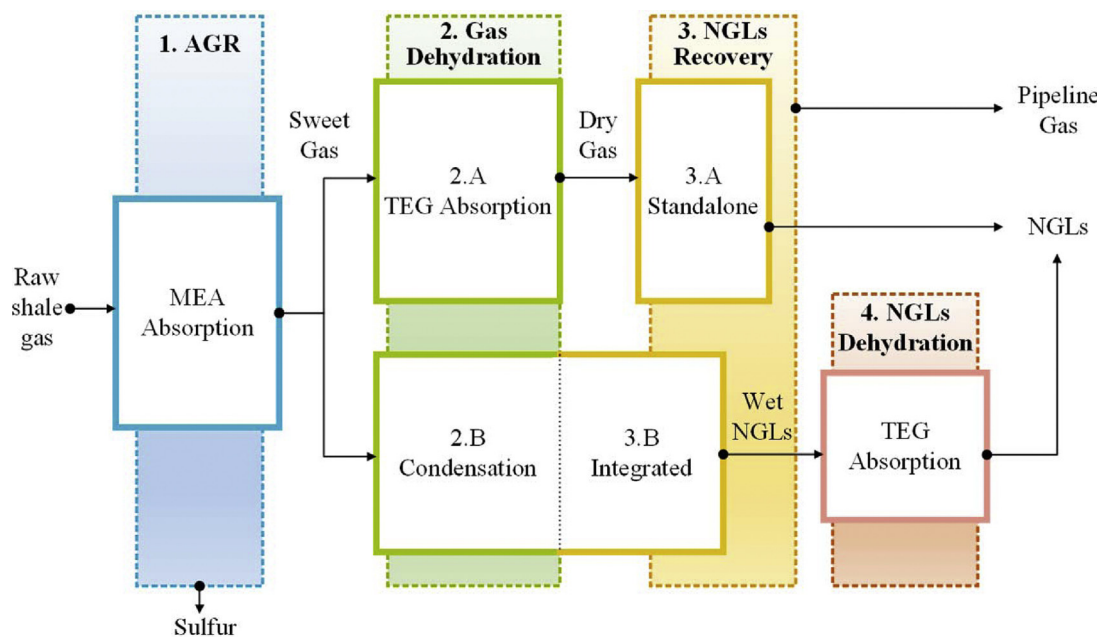


Fig. 3. Block flow diagram of two shale gas processing and NGLs recovery process systems. The processes in the conventional system and the proposed system are denoted by "A" and "B", respectively.

4.1. Acid gas removal

Hydrogen sulfide (H_2S) is toxic to human body and damages pipelines when it forms a corrosive acid in the presence of water (Mokhatab et al., 2006). Likewise, CO_2 corrodes pipelines when it meets water. In addition, a large amount of CO_2 in the NGLs recovery process will cause solids formation in cryogenic processes (Kidnay et al., 2011b). As shown in Table 1, the concentrations of H_2S and CO_2 in the pipeline gas should be lower than 2 vol% and 6 mg/m³, respectively. Furthermore, if NGLs recovery is employed in the subsequent sections, even lower concentrations are desired. There are multiple technologies for the removal of acid gases and the most well-established one is amine absorption (Rufford et al., 2012). We consider MEA absorption in the AGR section.

As shown in Fig. 4, a raw shale gas feed is introduced into the bottom of an absorber (T-100) and the acid gases are absorbed by a lean amine solution (Stream 113) from the top of the absorber. The treated gas, or sweet shale gas, leaves the top of the tower and is sent to the next section. The rich amine solution (Stream 101) is first depressurized to remove dissolved hydrocarbons, and then fed to a stripper (T-101) after being preheated in a heat exchanger. The liquid product leaves the bottom of the stripper and serves as the lean amine stream after it is cooled and pressurized. The gas product (Stream 107) containing primarily H_2S and CO_2 is sent to a sulfur recovery process. If the CO_2/H_2S ratio of the waste gas is high, sulfur cannot be recovered directly using a Claus process (He and You, 2015). To address this problem, an acid gas enrichment process is used to concentrate H_2S before it can be handled by a Claus process. A selective solvent of methyl-diethanolamine, or MDEA, is employed to concentrate H_2S in the gas mixture. MDEA is a tertiary amine, which reacts with CO_2 via a slow hydrolysis mechanism. This mechanism relies on a carbamate formation reaction and is regarded liquid-phase limited. In contrast, H_2S can react with MDEA through a direct proton-transfer reaction and considered gas-phase limited (Kidnay et al., 2011b). As a result, its selectivity of H_2S is much higher than that of CO_2 . The absorber-stripper cycle for concentrating H_2S is similar to that for separating the acid gases. The resulting H_2S concentration can reach 75% by volume. Next, 34% of the concentrated gas product is split to Stream

128 and the H_2S within this stream is converted to SO_2 in R-100 with abundant supply of air. The resulting SO_2 then reacts with the remaining gas product to generate solid sulfur, while the residual SO_2 content from R-101 is further treated by a shell Claus off-gas treating (SCOT) process. The equipment units in the SCOT process include two coolers (E-108 and E-109), a hydrogenator (R-102), a flash drum (V-102), and an absorber (T-104). In T-104, a lean MDEA solution of Stream 126 contacts with the gas product from V-101 countercurrently, and the H_2S , which is converted from SO_2 in R-102, is absorbed in the MDEA solvent and merges with the rich MDEA solution from T-102. The off-gas streams are sent to a combustor to generate electricity.

4.2. Dehydration and NGLs recovery in the conventional system

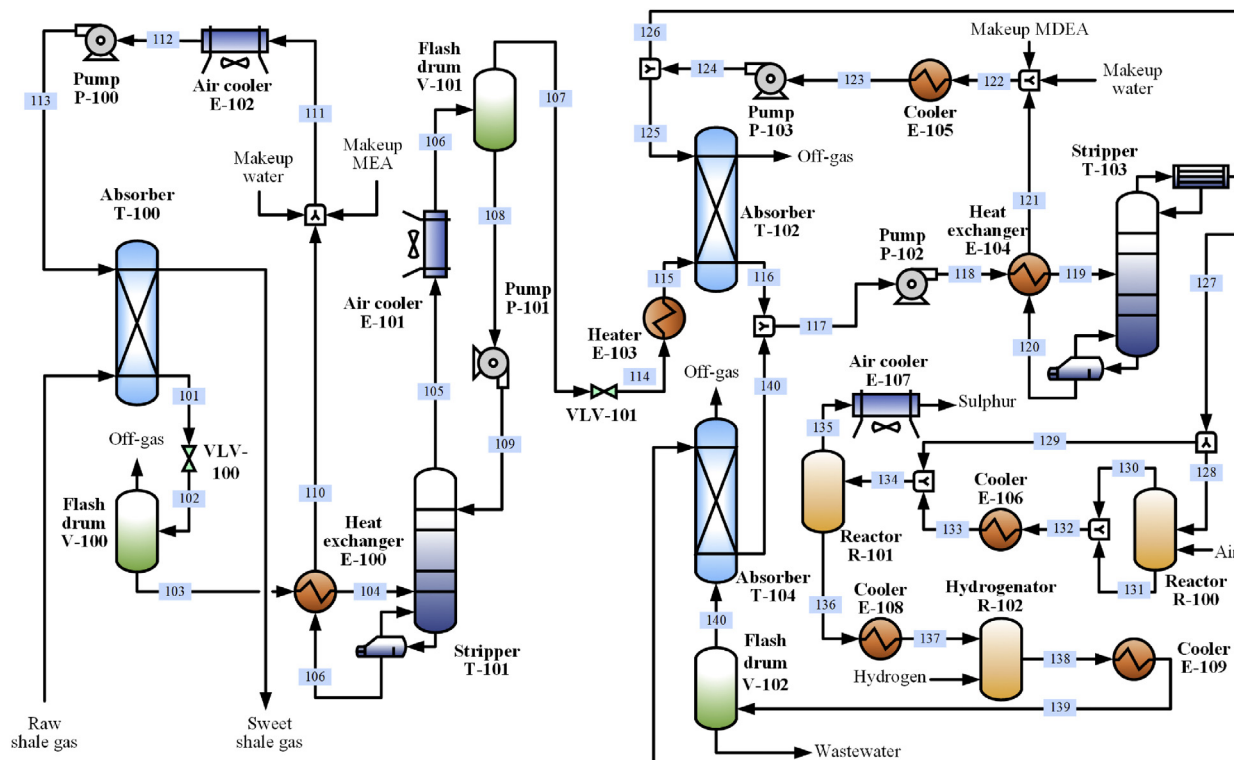
The sweet shale gas stream from the AGR section is water-saturated. However, operating cryogenic units in NGLs recovery and transporting gas product in pipelines require a low moisture concentration of 0.1 ppmv and 60 mg/m³, respectively. The reason for such a low concentration is to prevent the formation of hydrates and the condensation of free water (Gao and You, 2015c). Several technologies are available for gas dehydration, such as liquid desiccant dehydration, solid desiccant dehydration, and condensation (Kidnay et al., 2011a). In the conventional system, TEG absorption is employed as it is widely used in the gas processing industry. TEG shows high absorption efficiency, less energy-intensive regeneration, nontoxicity, and no interaction with the hydrocarbons.

As shown in Fig. 5, the sweet shale gas from the last section is fed to a phase separator to remove any free liquid, and the resulting gas stream then contacts with a lean TEG stream countercurrently. Most dry shale gas from the top of T-200 is introduced to the NGLs recovery section, while a small portion (0.15%) of the dry shale gas is used as the stripping gas in stripper T-202. The rich TEG stream from the bottom of T-200 is depressurized and flashed to remove most hydrocarbons, and the remaining solution is introduced into a stripper T-201, where most water in the rich TEG stream is rejected. The lean TEG solution is regenerated after the remaining water is removed in T-202, and the remaining hydrocarbons are removed in V-202.

Table 1

Intermediate and intensified product specifications (upper bounds unless specified). HHV is short for higher heating value.

	Values	Units	References
Feed to NGLs recovery			
CO ₂	50	ppmv	(Kidnay et al., 2011a)
H ₂ S	4	ppmv	(Kidnay et al., 2011a)
H ₂ O	0.1	ppmv	(Kidnay et al., 2011a)
Pipeline gas product			
CO ₂	2	vol%	(GPSA, 2012)
H ₂ S	6	mg/m ³	(GPSA, 2012)
H ₂ O	60	mg/m ³	(GPSA, 2012)
N ₂	3	vol%	(GPSA, 2012)
HHV lower bound	35.40	MJ/m ³	(GPSA, 2012)
HHV upper bound	42.80	MJ/m ³	(GPSA, 2012)
NGLs product (Y-grade)			
CO ₂	500	ppmv	(energytransfer.com)
CH ₄	0.50	vol%	(energytransfer.com)
CH ₄ /C ₂ H ₆	1.50	vol%	(energytransfer.com)
H ₂ O	10	ppmm	(GPSA, 2012)

**Fig. 4.** Process flowsheet of the AGR section.

Subsequently, the dry shale gas is fed to a NGLs recovery process in order to separate valuable NGLs. The dry gas is cooled to -15°C in the cold box E-300, and then the gas phase stream 303 is split into two streams. Stream 304 possesses 70% of the cooled dry gas and it is further cooled by a heat exchanger, a cooler, and a Joule-Tomson valve to reach -96.8°C . A flash drum immediately separates the gas product which contains over 98% of the methane by volume, while the liquid product is fed to the first stage of the demethanizer T-300. Stream 317 contains the remaining cooled dry gas and it is introduced into a turboexpander K-302, which generates electricity and drives a compressor K-300. The depressurized gas reaches -39.1°C and is fed to the 3rd tray of the demethanizer. A side draw cycle comprised of Streams 319 and 320 is employed in this design to enhance cooling efficiency (Getu et al., 2013). For transportation purpose, pipeline gas is pressurized to 60 bar via a

multi-stage compression system. The NGLs product obtained from the bottom of T-300 is pressurized to 600 psig.

4.3. Dehydration and NGLs recovery in the proposed system

Among gas dehydration technologies, condensation processes are also widely recognized and applied (Minkkinen et al., 1998; Netusil and Ditzl, 2011). Almost all water vapor can condense from the sweet shale gas if it is cooled to -70°C at 41 bar. Since the shale gas will be ultimately cooled to about -98°C for NGLs recovery, gas dehydration via a condensation process can be accomplished naturally and conveniently. Compared with the absorption technology, a condensation process does not require multiple columns for absorption and solvent recovery. Furthermore, there is no need to split a stream of dry gas as the stripping gas. However, to prohibit the formation of ice and hydrate, a large amount of inhibitor materi-

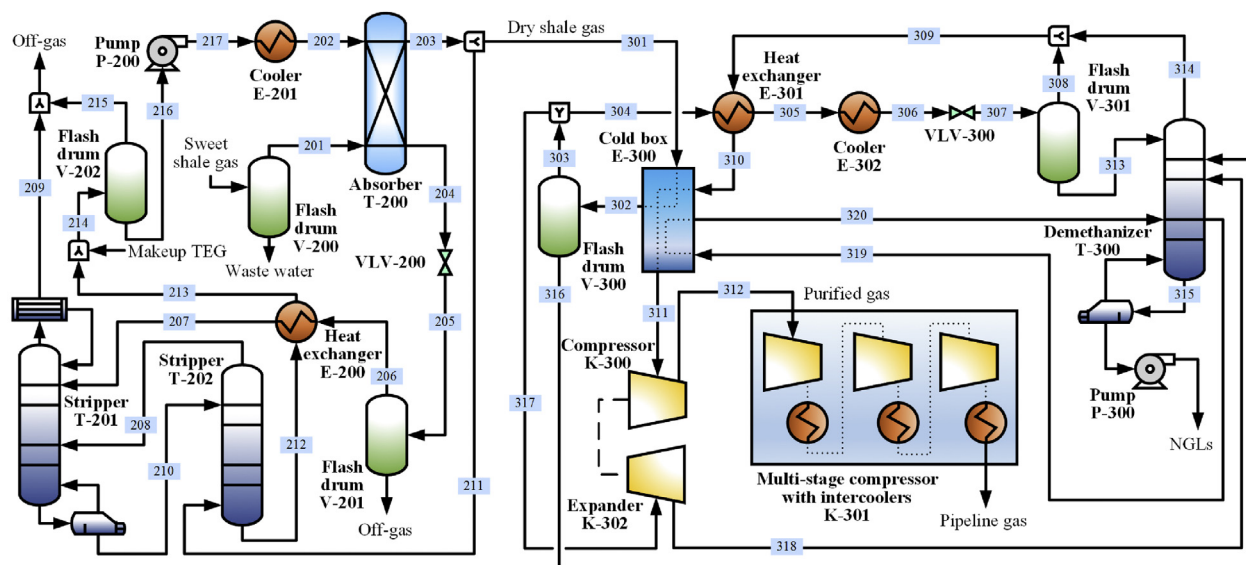


Fig. 5. Process flowsheet of the gas dehydration and NGLs recovery sections in the conventional system.

als must be injected into the system and thus incur extra separation costs. In the natural gas processing industry, the condensation technology is usually used for natural gas with little NGLs (Esteban et al., 2000). If the existing process designs are used to process shale gas with more NGLs, there will be two outcomes. First, the gas product will be mixed with a significant amount of NGLs and the HHV of the gas product is likely to exceed the upper bound in Table 1. Second, the condensate product (the remaining NGLs, originally designed to be used as fuels for energy generation) will contain too much methanol to be utilized in the downstream processes. In the literature, however, there is no condensation-based process design for processing shale gas containing a significant amount of NGLs.

One of the goals in this work is to develop a novel condensation-based process design that addresses the aforementioned issues of the existing designs. In the proposed process design, a demethanizer column based separation process is integrated in the design for more efficient separation of the pipeline gas product and NGLs. In addition, the undesired methanol in the NGLs product is separated and recycled by integrating an extraction process and TEG absorption process. As shown in Fig. 6, the sweet gas is cooled in an air cooler E-200 to 31 °C and then cooled in heat exchanger E-201 to 16 °C. Liquid products after each cooling are sent to extractor T-201. Next, the gas is mixed with methanol and the mixture is sent to two heat exchangers and a cooler to achieve -68 °C. After a three-phase separator, the light liquid product is sent to demethanizer T-200 and the heavy liquid product containing only water and methanol is sent to distillation column T-202. The gas product is free of water and methanol, and it is later cooled to -78 °C in E-205. With the liquid split and sent to T-200, the gas phase is introduced to expander K-200 and the temperature is ultimately reduced to -98 °C. The methane concentration in the gas stream 213 is 98.6% and the liquid stream 219 is injected onto the first tray of T-200. The gas product from T-200 is merged with stream 213 and serves as a coolant in E-205, E-203, and E-201. Pipeline gas is obtained after the gas product is pressurized by compressor K-201 and multi-stage compressor K-202. The liquid product from T-200 contains primarily NGLs and small amount of methanol (1.6%). As NGLs pipelines require a methanol concentration of less than 50 ppmv, we wash methanol off in extractor T-201 using condensed water 235 and 234, as well as recycling water 240. The water-methanol mixture is distilled in T-202 and the methanol product in the top is recycled and mixed with the sweet gas in stream 233.

To obtain qualified NGLs, wet NGLs are subsequently dehydrated through a TEG absorption process. Since the wet NGLs from the extractor are liquid, they are depressurized to become gas and heated to 27 °C before being sent to the absorber T-300. 99.95% of the dry NGLs are cooled by heat exchanger E-300 to -4.9 °C, and the resulting gas stream 307 is pressurized and converted to liquid at 30 bar. Later, stream 308 is cooled by heat exchanger E-301 and cooler E-302 before the liquid is pressurized to 600 psig. In addition, the resulting liquid stream 312 is directly pressurized to 600 psig and merged with stream 311 as the final NGLs product. The remaining solvent regeneration process is similar to the dehydration section of the conventional system.

5. Case studies

In this section, the proposed simulation-based process intensification method to hedge against uncertain feedstock compositions is illustrated by case studies regarding the conventional and novel shale gas processing systems. The case studies consider raw shale gas gathered and transported from multiple wellsites in the gulf coast region of the U.S. In the downstream, a natural gas power plant located in the same region will purchase and consume the pipeline gas from the processing facility. The goal is to develop and compare intensified process designs of both shale gas processing systems that can generate qualified products when the flow rates of raw shale gas from various wellsites are fluctuating.

5.1. Assumptions

Before parameters and results are presented, we show the major assumptions considered in the case studies:

- The gas demand of the downstream power plant can be fully fulfilled by processing the raw shale gas extracted from the considered wellsites during the lifespan of the processing facility.
- The compositions of the raw shale gas are stable overtime and their production rates are allowed to increase or decrease.
- In a region-wide shale gas compositions dataset (Allen et al., 2013), there are both dry wells that contain barely NGLs and wet wells that include a significant amount of NGLs. It is noted that the proposed approach can handle any combination of dry

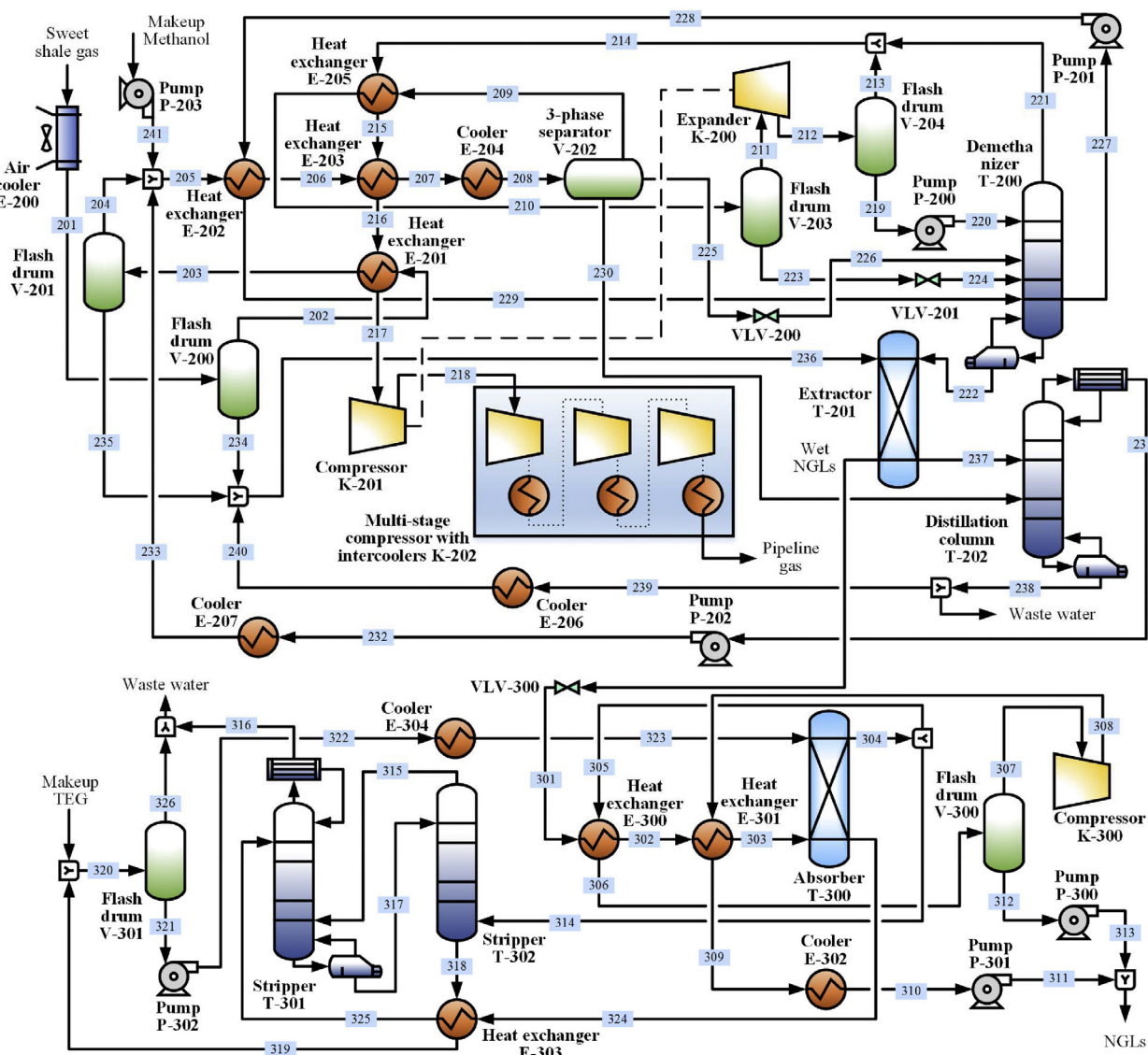


Fig. 6. Process flowsheet of the gas dehydration and NGLs recovery sections in the proposed system.

and wet wells. Without loss of generality, we assume half of the shale wells are dry wells the other half are wet wells.

- Trace components other than CH₄, C₂H₆, C₃H₈, C₄H₁₀, C₅₊ (represents the hydrocarbon molecules with more than 4 carbon atoms), CO₂, H₂S, N₂, and H₂O are ignored in the analysis.
- H₂S and H₂O concentrations are missing from the major composition source (Allen et al., 2013), so they are assumed fixed and the applied values represent the average level in this region (Pring, 2012).

5.2. Input parameters

The designed capacity of the natural gas power plant is 1150 MW (F. Power, 2016). Given an energy conversion efficiency of 51.5% as applied in the NETL baseline studies for fossil energy plants (Fout et al., 2015), a pipeline gas stream of 7619 MMBTU/h must be generated and sold to the power plant. Additionally, in the NETL report, a 641 MW natural gas power plant requires a natural gas supply of 97.5 MMSCFD (Fout et al., 2015). Following this result, approximately 174.9 MMSCFD natural gas is required for the studied natural gas power plant. As the average shale gas production rate of the middle- and large-size sampling wells in the gulf coast region

is 23 MMSCFD (Allen et al., 2013), there should be 8 shale wells in this region that serve as raw shale gas sources for the demand of pipeline gas. As mentioned in the assumption, we consider 4 dry wells and 4 wet wells.

There are 9 components considered in raw shale gas: CH₄, C₂H₆, C₃H₈, C₄H₁₀, C₅₊, CO₂, H₂S, N₂, and H₂O. The majority of the raw shale gas composition data are taken from the study of Allen et al. (Allen et al., 2013). However, no H₂S or H₂O concentration is mentioned in this study. In order to address the data gap, we fix the H₂S and H₂O concentrations as reported in a different report (Pring, 2012) and integrate the fixed concentration with the other compositions in (Allen et al., 2013). The final compositions and other properties of raw shale gas feedstocks are shown in Table 2. It is noted that all feedstock compositions, temperature, and pressure data are taken from literature (He and You, 2014; Allen et al., 2013; Pring, 2012; EIA, 2006) and the HHV values are evaluated using the compositions. Parameters used in the techno-economic analysis are shown in Table 3.

Although w_j can take any value between [0,1] as long as the sum of all w_j is equal to 1, it is impractical to test all feasible feedstock compositions in the last step of the proposed algorithm. We surveyed existing papers and found no more than 10 scenarios were

Table 2

Raw shale gas feedstock properties. Composition data are from (Allen et al., 2013; Pring, 2012); Temperature is from (He and You, 2014); Pressure is from (EIA, 2006).

	Feed #1	Feed #2	Feed #3	Feed #4	Feed #5	Feed #6	Feed #7	Feed #8
Composition (mole%)	CH ₄	94.64	95.62	95.75	94.81	79.9	78.48	72.62
	C ₂ H ₆	0.05	0.08	0.08	0.16	11.61	12.68	14.47
	C ₃ H ₈	0	0	0	0	3.98	4.44	6.37
	C ₄ H ₁₀	0	0	0	0	2.12	2.11	3.42
	C ₅₊	0	0	0	0	1.22	1.02	1.59
	CO ₂	4.93	3.92	3.78	4.46	0.73	0.86	1.11
	H ₂ S	0.23	0.23	0.23	0.23	0.23	0.23	0.23
	N ₂	0.03	0.04	0.04	0.22	0.09	0.06	0.07
	H ₂ O	0.12	0.12	0.12	0.12	0.12	0.12	0.12
HHV (MJ/m ³)		35.62	36.01	36.06	35.76	45.83	46.12	49.36
Temperature (°C)		35						45.00
Pressure (psig)		600						

Table 3

Parameters in techno-economic analysis.

Parameters	Values	Units	Parameters	Values	Units
Raw shale gas price	1.80	\$/MMBTU	Low pressure steam	1.90	\$/GJ
Hydrogen price	1.76	\$/kg	Middle pressure steam	2.20	\$/GJ
Methanol	0.60	\$/kg	High pressure steam	2.50	\$/GJ
Solvent (MEA, DEA, TEG) price	2.70	\$/kg	Fired heat (1000 °C)	4.25	\$/GJ
Process water price	0.20	\$/tonne	Electricity price	0.07	\$/kWh
Cooling water	0.21	\$/GJ	Indirect cost coefficient	32%	
Refrigerant 1 (-103 °C)	8.53	\$/GJ	Operating time	8000	h/year
Refrigerant 2 (-25 °C)	2.74	\$/GJ	Interest rate	15%	
Low pressure steam generation	-1.89	\$/GJ	Life span	20	year
Middle pressure steam generation	-2.19	\$/GJ	CEPCI 2009	521.9	
High pressure steam generation	-2.49	\$/GJ	CEPCI 2015	537.1	

Table 4

Weights and compositions (mole%) of Feeds #9–#18.

	Feed #9	Feed #10	Feed #11	Feed #12	Feed #13	Feed #14	Feed #15	Feed #16	Feed #17	Feed #18
Weights										
Feed #1	0.0253	0.1699	0.1600	0.0266	0.0515	0.1351	0.1536	0.0644	0.0274	0.0588
Feed #2	0.0614	0.1594	0.0783	0.0252	0.0977	0.0930	0.0298	0.3743	0.2925	0.1012
Feed #3	0.1343	0.0522	0.2565	0.1983	0.0285	0.1317	0.1369	0.1127	0.0204	0.1574
Feed #4	0.1758	0.0711	0.1299	0.1223	0.1811	0.1907	0.0445	0.2121	0.0918	0.1560
Feed #5	0.2007	0.1573	0.1046	0.1720	0.1613	0.0677	0.1617	0.0922	0.2564	0.1491
Feed #6	0.2744	0.2105	0.1474	0.2054	0.2005	0.1197	0.1876	0.0041	0.0734	0.1462
Feed #7	0.0684	0.1185	0.0678	0.2128	0.2555	0.0946	0.0984	0.0707	0.1399	0.1038
Feed #8	0.0597	0.0612	0.0556	0.0374	0.0240	0.1674	0.1876	0.0695	0.0982	0.1275
Compositions (mole%)										
CH ₄	85.17	85.71	88.85	83.86	83.23	87.62	84.70	91.24	85.58	86.36
C ₂ H ₆	7.51	6.92	4.74	8.13	8.42	5.59	7.79	2.99	7.06	6.55
C ₃ H ₈	2.69	2.56	1.72	3.10	3.26	2.06	2.84	1.11	2.62	2.40
C ₄ H ₁₀	1.34	1.29	0.86	1.59	1.68	1.01	1.40	0.57	1.35	1.20
C ₅₊	0.69	0.65	0.44	0.79	0.83	0.51	0.72	0.29	0.70	0.62
CO ₂	2.16	2.45	2.97	2.09	2.14	2.77	2.13	3.36	2.25	2.43
H ₂ S	0.23	0.23	0.23	0.23	0.23	0.23	0.23	0.23	0.23	0.23
N ₂	0.09	0.07	0.08	0.08	0.09	0.09	0.08	0.09	0.08	0.09
H ₂ O	0.12	0.12	0.12	0.12	0.12	0.12	0.12	0.12	0.12	0.12

used in rigorous simulation-based design validation (Getu et al., 2013; Wang and Xu, 2014). As shown in Table 4 we develop 10 randomly generated feedstock compositions (Feeds #9–#18) based on the compositions of Feeds #1–#8. In order to obtain the new compositions, we first generate 10 sets of weights for the 10 generated feedstock compositions, respectively. Next, we calculate new compositions as the products of the weights and corresponding original compositions.

5.2. Mass and energy balance of the deterministic designs

The mass balance results of the 8 deterministic designs based on the proposed process system are given in Table 5. The flow rates of raw shale gas in deterministic designs #1–#4 are approximately 190 MMSCDF, while those in deterministic designs #5–#8

are notably larger. This is because the feedstocks from wellsites #1–#4 are “dry” shale gas and nearly all feed gas remains in the pipeline gas products. In contrast, the feedstocks from wellsites #5–#8 are “wet” shale gas and a portion of the feedstock is separated as an NGLs product. In order to satisfy the downstream pipeline gas demand, more feedstocks are processed in deterministic designs #5–#8. Hydrogen is consumed in the sulphur recovery process and it reacts with surplus sulphur dioxide (He and You, 2014). Since the feed flow rates in deterministic designs #5–#8 are higher, there are more sulphur products and the hydrogen consumption rates are also higher. With more NGLs in the feedstock, raw shale gas from wellsites #5–#8 is able to dissolve more MEA than shale gas from wellsites #1–#4. Therefore, the MEA consumption rates are higher in the deterministic designs with “wet” shale gas feeds. The MDEA consumption rates are associated with

Table 5

Mass balance results of the deterministic designs based on the proposed process system.

	Design #1	Design #2	Design #3	Design #4	Design #5	Design #6	Design #7	Design #8
Input								
Raw shale gas (MMSCDF)	191.80	189.73	189.45	191.06	222.18	225.79	242.56	219.26
Hydrogen (kg/h)	2.43	2.42	2.41	2.42	2.83	2.86	3.05	2.79
MEA (kg/h)	3.92	3.90	3.90	3.91	11.70	13.11	16.73	11.93
MDEA (kg/h)	0.48	0.40	0.39	0.44	0.21	0.23	0.26	0.21
Methanol (kg/h)	22.98	22.71	22.68	22.87	0.17	0.56	0.64	0.51
TEG (kg/h)	0.00	0.00	0.00	0.00	0.04	0.04	0.05	0.03
Process water (tonne/h)	0.86	0.73	0.66	0.75	0.50	0.58	0.65	0.53
Output								
Pipeline gas (MMSCDF)	181.58	181.54	181.54	181.78	179.88	179.65	179.15	180.00
NGLs (tonne/h)	0.00	0.00	0.00	0.00	77.90	83.14	119.63	70.43
Sulfur (tonne/h)	0.69	0.69	0.69	0.69	0.80	0.81	0.87	0.79
Direct emissions								
CO ₂ (tonne/h)	20.96	16.54	15.88	18.94	3.81	4.54	6.27	4.03
SO ₂ (kg/h)	6.30	7.65	7.35	8.66	1.83	1.96	2.45	1.90
H ₂ S (kg/h)	8.42	4.64	4.35	6.47	10.22	13.36	23.38	11.23

the amount of acid gases in the feedstocks, and thus deterministic designs #1–#4 generally consume more MDEA solvent. Deterministic designs #5–#8 achieve more thorough separation of water than deterministic designs #1–#4, because NGLs recovery requires a much lower water concentration in the dry shale gas. As the attraction force between water and methanol molecules is rather strong, much more methanol is lost in the pipeline gas in deterministic designs #1–#4. TEG adsorption appears only in deterministic designs #5–#8 and the size of this process is much smaller than the other processes. As a result, only a slight amount of the TEG solvent is lost. In contrast to the feed flow rates, pipeline gas flowrates are quite close among all deterministic designs. The small differences stem from the variations in the resulting pipeline gas compositions. We find that raw shale gas from wellsite #7 has the largest portion of NGLs in the feedstock.

The energy balance results of the 8 deterministic designs based on the proposed process system are shown in Table 6. As mentioned in the Uncertainty in Feedstock Compositions section, the pipeline gas product is to meet the fuel demand of a natural gas power plant. Therefore, the energy flow rates of all pipeline gas must be at least 7,619.0 MMBTU/h. Nearly all raw shale gas in deterministic designs #1–#4 remains in the pipeline gas, so the energy flow rates in these feedstocks can be lower than those in deterministic designs #5–#8. With one more section to separate NGLs, most utility consumption rates in deterministic designs #5–#8 are higher than those in deterministic designs #1–#4. One exception comes from the MP steam consumption rates. More acid gases are present and need to be removed in raw shale gas from wellsites #1–#4, so a stream of MEA absorbent with over 4 times higher flow rates is recirculated in the AGR sections in deterministic designs #1–#4. As a result, much more MP steam is consumed in stripping column T-101 for solvent regeneration. The mass and energy balance results of the 8 deterministic designs based on the conventional process system are presented in Appendix B.

5.3. Capacity-oriented process intensification

In the second step of the proposed method, there are two essential components for the development of an intensified design. We first determine the equipment capacities and associated direct costs. Given similar operating temperatures and pressures among the deterministic designs (in Table 7), the equipment direct cost of a unit is positively correlated with its capacity. The breakdown of total direct cost in all 16 deterministic designs and 2 intensified designs are shown in Fig. 7. The total direct costs of deterministic designs #1–#4 of the conventional system are slightly lower

than those of the proposed system, while the total direct costs of deterministic designs #5–#6 of the conventional system are higher than those of the proposed system. The most significant difference comes from processing raw shale gas of wellsite #7 and the total direct cost of the conventional system is 2.25 times that of the proposed system. Intensified designs show higher total direct costs than any of the associated deterministic designs. The intensified design of the conventional system is 1.83 times as expensive as the intensified design of the proposed system.

With a closer look into the breakdown results, we find that in deterministic designs #1–#4, the direct cost of the AGR section contributes to more than 50% of the total direct cost. Since the NGLs in the raw shale gas from wellsites #1–#4 are ignorable, the NGLs recovery costs in deterministic designs #1–#4 of the conventional system account for only the compressor system. The integrated process in the proposed system shows a higher direct cost than the sum of direct costs of dehydration and NGLs recovery in the conventional system. With less acid gases to remove in the raw shale gas from wellsites #5–#8, the direct cost of AGR section reduces approximately 60%. Since the sweet gas from the AGR section is water-saturated, the water concentrations of the sweet gas streams from various designs are identical. Consequently, the difference in the amount of water to be separated depends primarily on the flow rate of the sweet gas stream. As there are insignificant differences among the flow rates of the sweet gas streams, the variations of the direct costs for dehydration are not as pronounced as those of other sections. On the contrary, both NGLs recovery in the conventional system and integrated process in the proposed system become considerably more expensive when they are used to process the raw shale gas from wellsites #5–#8. Furthermore, the direct cost of the NGLs recovery process is a lot more sensitive to the amount of NGLs in the feedstock than the direct cost of integrated process in the proposed system. For the raw shale gas from wellsite #8, the direct cost of the dehydration and NGLs recovery process in the conventional system is only 11% higher than the direct cost of integrated process in the proposed system. However, this value increases remarkably to 166% for the raw shale gas from wellsite #7. The direct costs of the subprocesses in the intensified designs are higher than the corresponding direct costs in the deterministic designs.

Next, we provide a conservative estimation of the operating conditions when uncertainty in feedstock composition is realized. The operating cost is the sum of the feedstock cost and the utility cost. The feedstock cost is a linear function of the energy flow rate of raw shale gas. As shown in Table 6, deterministic design #7 has the largest feedstock energy flow rate, thus the highest feedstock cost. The breakdown of utility costs in all 16 deterministic designs is

Table 6

Energy balance results of the deterministic designs based on the proposed process system.

	Design #1	Design #2	Design #3	Design #4	Design #5	Design #6	Design #7	Design #8
Feed ($\times 10^3$ MMBTU/h)								
Raw shale gas	7.63	7.62	7.62	7.62	11.36	11.62	13.36	11.01
Utility (GJ/h or specified)								
Electricity (MW)	5.25	5.14	5.12	5.21	9.84	10.27	11.57	9.73
Cooling Water	137.97	135.78	135.37	137.17	39.54	40.13	42.51	39.22
Refrigerant 1	0.00	0.00	0.00	0.00	55.18	60.72	83.17	53.29
Refrigerant 2	0.02	0.02	0.02	0.02	13.76	14.65	22.05	12.33
LP Steam Generation	2.73	2.56	2.52	2.65	15.14	15.38	25.68	15.07
MP Steam Generation	0.20	0.19	0.19	0.19	0.00	0.00	0.00	0.00
HP Steam Generation	5.11	4.93	4.89	5.03	4.85	4.94	5.30	4.79
LP Steam	0.00	0.00	0.00	0.00	27.16	32.03	40.01	26.30
MP Steam	308.90	294.71	293.74	305.71	49.46	58.81	67.33	51.00
HP Steam	0.00	0.26	0.26	0.27	17.28	0.38	0.58	16.69
Fired Heat	11.90	11.40	11.27	11.68	10.57	10.77	11.60	10.44
Products ($\times 10^3$ MMBTU/h or specified)								
Pipeline gas	7.62	7.62	7.62	7.62	7.62	7.62	7.62	7.62
NGLs	0.00	0.00	0.00	0.00	3.74	4.00	5.74	3.39
Sulfur (MMBTU/h)	6.01	5.97	5.96	5.99	6.98	7.07	7.53	6.88

Table 7

Operating conditions of key operating units in the deterministic designs based on the proposed process system. In each cell, the first value represents the lower bound, and the second value represents the upper bound.

	Design #1	Design #2	Design #3	Design #4	Design #5	Design #6	Design #7	Design #8
T-100 P(bar)	42.0, 42.4	42.0, 42.4	42.0, 42.4	42.0, 42.4	42.0, 42.4	42.0, 42.4	42.0, 42.4	42.0, 42.4
T-100 T(°C)	37.3, 90.9	37.3, 96.1	37.3, 96.9	37.3, 92.2	37.8, 55.9	38.7, 59.6	40.4, 66.1	38.2, 58.3
T-101 P(bar)	1.9, 2.0	1.9, 2.0	1.9, 2.0	1.9, 2.0	1.9, 2.0	1.9, 2.0	1.9, 2.0	1.9, 2.0
T-101 T(°C)	112.6, 122.3	113.8, 122.4	113.9, 122.4	113.1, 122.3	99.1, 121.7	106.3, 121.9	103.0, 122.0	100.2, 121.7
T-102 P(bar)	0.6, 0.7	0.6, 0.7	0.6, 0.7	0.6, 0.7	0.6, 0.7	0.6, 0.7	0.6, 0.7	0.6, 0.7
T-102 T(°C)	30.4, 34.4	30.3, 33.9	30.3, 33.7	30.3, 34.2	30.2, 36.1	30.3, 36.6	30.4, 37.2	30.3, 36.3
T-103 P(bar)	1.5, 1.6	1.5, 1.6	1.5, 1.6	1.5, 1.6	1.5, 1.6	1.5, 1.6	1.5, 1.6	1.5, 1.6
T-103 T(°C)	57.9, 117.2	58.9, 117.2	59.4, 117.2	58.3, 117.2	62.1, 117.2	60.5, 117.2	59.7, 117.2	61.1, 117.2
T-104 P(bar)	1.0, 1.1	1.0, 1.1	1.0, 1.1	1.0, 1.1	1.0, 1.1	1.0, 1.1	1.0, 1.1	1.0, 1.1
T-104 T(°C)	30.1, 31.6	30.1, 31.4	30.1, 31.3	30.1, 31.5	30.1, 32.3	30.1, 32.4	30.1, 32.5	30.1, 32.3
T-200 P(bar)	N/A	N/A	N/A	N/A	22.5, 23	22.5, 23	22.5, 23	22.5, 23
T-200 T(°C)	N/A	N/A	N/A	N/A	−97.1, 21.5	−96.2, 20.0	−94.0, 25.0	−97.6, 20.0
T-201 P(bar)	N/A	N/A	N/A	N/A	22.5, 23.0	22.5, 23.0	22.5, 23.0	22.5, 23.0
T-201 T(°C)	N/A	N/A	N/A	N/A	22.0, 23.1	20.5, 21.7	25.4, 26.4	20.3, 21.6
T-202 P(bar)	27.8, 28.3	27.8, 28.3	27.8, 28.3	27.8, 28.3	22.0, 23.0	22.0, 23.0	22.0, 23.0	22.0, 23.0
T-202 T(°C)	189.5, 231.3	189.5, 231.3	189.5, 231.3	189.5, 231.3	172.6, 220.1	172.7, 220.1	173.3, 220.1	172.8, 220.1
T-300 P(bar)	N/A	N/A	N/A	N/A	5.0, 5.1	5.0, 5.1	5.0, 5.1	5.0, 5.1
T-300 T(°C)	N/A	N/A	N/A	N/A	25.6, 25.7	25.6, 25.7	25.6, 25.7	25.6, 25.7
T-301 P(bar)	N/A	N/A	N/A	N/A	1.0, 1.1	1.0, 1.1	1.0, 1.1	1.0, 1.1
T-301 T(°C)	N/A	N/A	N/A	N/A	76.6, 200.0	75.8, 200.0	79.0, 200.0	75.4, 200.0
T-302 P(bar)	N/A	N/A	N/A	N/A	1.1, 1.2	1.1, 1.2	1.1, 1.2	1.1, 1.2
T-302 T(°C)	N/A	N/A	N/A	N/A	188.3, 196.1	188.0, 196.0	188.2, 196.1	188.6, 196.2

shown in Fig. 8. We find that the utility cost of deterministic design #7 is higher than that of other deterministic designs. Therefore, we adopt the operating conditions of deterministic design #7 in the intensified designs. In Fig. 8, the electricity cost of the proposed system is always higher than that of the conventional system. This results from the utilization of an expander in the proposed system and more electricity is consumed in the proposed system to recover the pressure drop. As analyzed in the energy balance results, heating utilities are mainly consumed in the AGR section, so the heating cost is higher in deterministic designs #1–#4 than in deterministic designs #5–#8, and the difference in the heating cost of the conventional system and the proposed system is small. On the contrary, cooling utilities, especially refrigerants, are mainly used in the NGLs recovery and condensation processes. Therefore, the cooling costs in deterministic designs #1–#4 are ignorable compared with those in deterministic designs #5–#8. We also find that the integrated process in the proposed system shows a higher cooling cost than NGLs recovery process due to the separation of methanol solvent from a water-methanol mixture. As much methanol is lost in deterministic designs #1–#4 of the proposed system, they show relatively high solvent costs among all deterministic designs.

As mentioned previously, the intensified designs involve two groups of major decisions. As the operating conditions can be tailored to the feedstock, the operating cost of each section ends up being proportional to the flow rates of the components to be removed. Therefore, the overall economic performance is primarily influenced by equipment utilization efficiencies. The equipment utilization efficiencies for processing Feed #7 in the intensified process systems are shown in Fig. 9. Although the operating conditions are relatively conservative compared with those for processing other feedstocks, a number of equipment units are still operated below their capacities. More specifically, most equipment units in the dehydration and NGLs recovery sections operate near or at their capacities, while the utilization efficiencies in the acid gas removal section are relatively lower. This results stem from the fact that Feed #7 contains leaner acid gases but richer NGLs. It is also expected that if the flow rate of the feedstock is lower than those in Table 5, most bars in Fig. 9 will be shorter than the bars for 100%.

The overall economic evaluation results based on the proposed system are shown in Table 8 and those of the conventional system are shown in Appendix B. The intensified design of the conventional system shows higher investment cost and a lower operating cost,

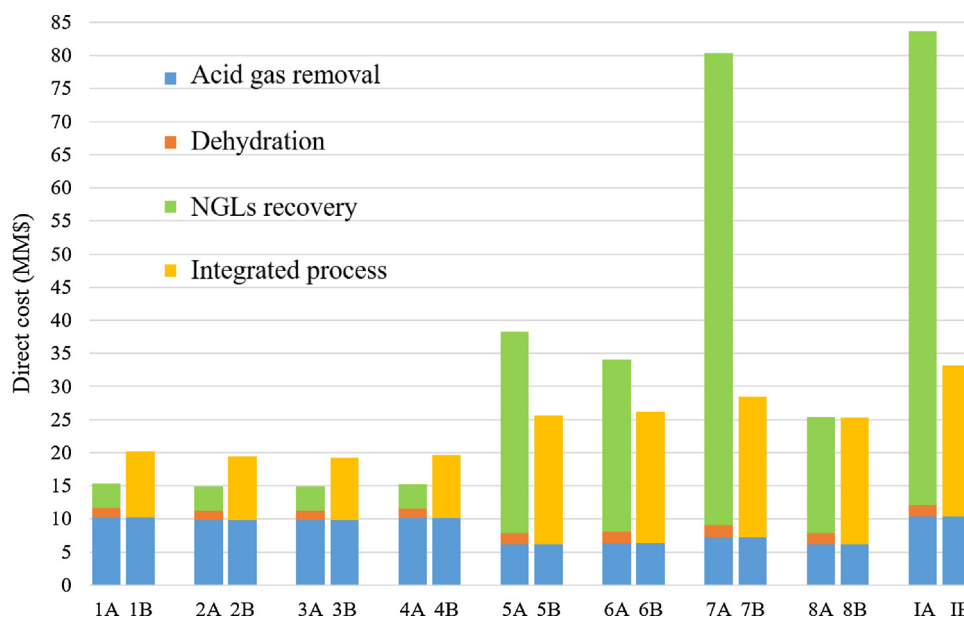


Fig. 7. Breakdown of total direct costs of deterministic and intensified designs. Each bar is noted by a two characters. The first character represents the type of designs: numbers denote the deterministic designs and “I” denotes the intensified designs. The second character represents process systems: “A” is the conventional process system and “B” is the proposed process system.

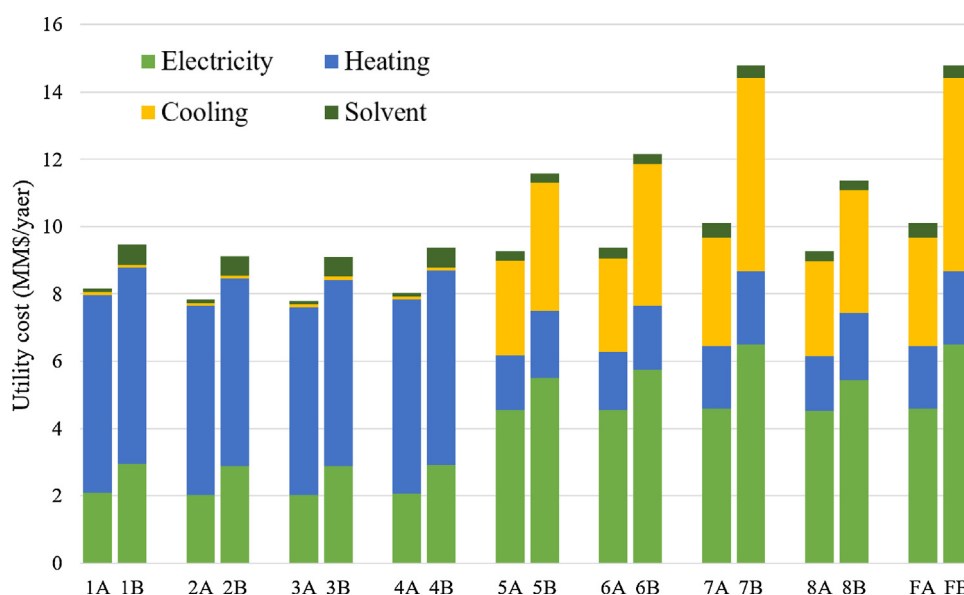


Fig. 8. Breakdown of operating costs of deterministic and intensified designs. Each bar is noted by a two characters. The first character represents the type of designs: numbers denote the deterministic designs and “I” denotes the intensified designs. The second character represents process systems: “A” is the conventional process system and “B” is the proposed process system.

Table 8

Economic evaluation results based on the proposed system.

	Design #1	Design #2	Design #3	Design #4	Design #5	Design #6	Design #7	Design #8	Intensified Design
Total direct cost (MM\$)	20.23	19.47	19.29	19.72	25.62	26.14	28.47	25.26	33.22
Indirect cost (MM\$)	6.47	6.23	6.17	6.31	8.20	8.37	9.11	8.08	10.63
Feedstock cost (MM\$/year)	109.84	109.82	109.82	109.83	163.69	167.43	192.45	158.60	192.45
Utility cost (MM\$/year)	9.46	9.13	9.10	9.38	11.57	12.15	14.80	11.36	14.80
Total annualized cost (MM\$/year)	123.57	123.06	122.99	123.37	180.67	185.09	213.26	175.29	214.26
Unit annualized cost (\$/MMBTU)	2.03	2.02	2.02	2.02	1.99	1.99	2.00	1.99	2.00

while the intensified design of the proposed system shows a lower investment cost and higher operating cost. In both designs, the feedstock costs dominate the total annualized costs. In the intensified design of the proposed system, the unit annualized cost per

MMBTU energy in the raw shale gas is \$2.00, which is 12% higher than the raw shale gas price. In comparison, the unit annualized cost of the intensified design of the conventional system is \$2.06 (from Table B3). Therefore, from the standpoint of an economic

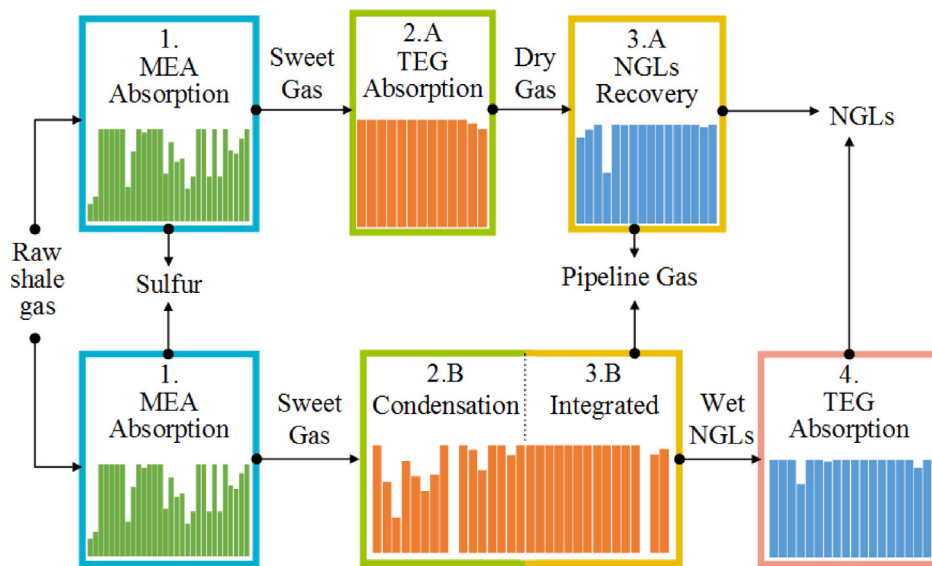


Fig. 9. Equipment utilization efficiency distributions of the intensified conventional process design (with "A") and the intensified proposed process design (with "B") when Feed #7 is processed. Each bar represents the utilization efficiency of one equipment unit. The maximum height in each distribution represents 100% utilization.

— 1B — 2B — 3B — 4B — 5B — 6B — 7B — 8B — IB — Upper Bound

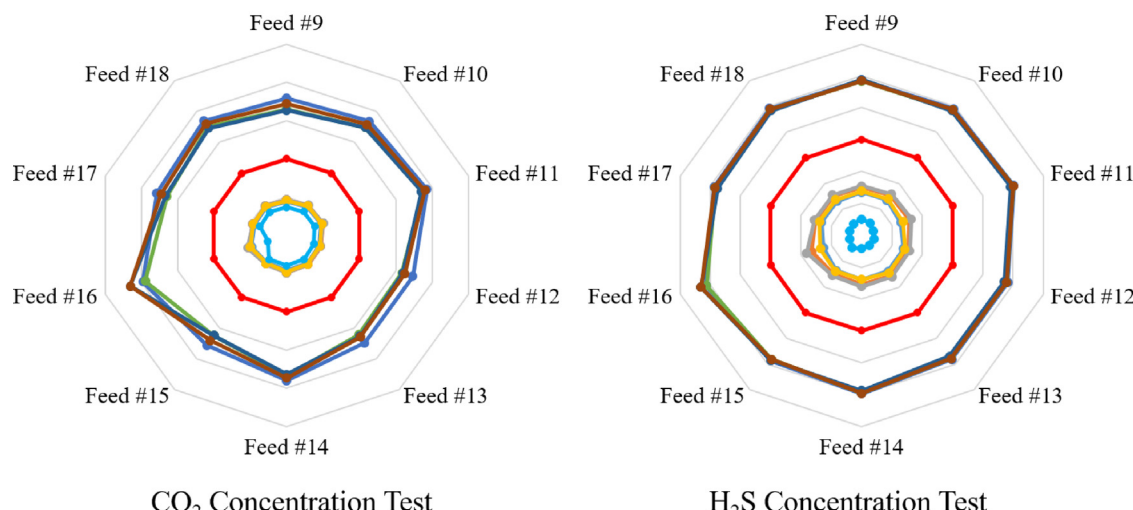


Fig. 10. CO_2 and H_2S concentration test results for the deterministic and intensified designs based on the proposed process system. Each performance profile is noted by a two characters. The first character represents the type of designs: numbers denote the deterministic designs and "I" denotes the intensified designs. The second character is "B", which denotes the proposed process system.

analysis, the intensified design of the proposed system is a more cost-effective design.

It is worth mentioning that by adjusting operating conditions, the intensified designs are able to process feedstocks with lower flow rates and still generate qualified pipeline-quality products. In this specific case study, we aim to satisfy a downstream power plant with a predetermined demand, so the feed flow rate could be maintained at a similar level by completing more wells over time.

5.4. Design validation

In order to validate the obtained designs (both deterministic and intensified), they are used to process a series of randomly generated feedstocks in Table 4. Since the nitrogen concentrations in the considered feedstocks are already lower than the upper bound, we consider the other four criteria in Table 1: CO_2 concentration, H_2S concentration, H_2O concentration, and HHV. The test results are

shown in Fig. 10 and Fig. 11. Each sub-figure is a radar chart and shows the test results of one criterion. The axes represent various feedstock compositions and each polygon denotes the performance profile of a design. Each point on a performance profile corresponds to the result regarding a certain feedstock and a certain design. The red polygons stand for the upper bounds of the tested values. As a result, a performance profile partially or entirely outside the red polygons is considered not passing the design validation.

In Fig. 10 and Fig. 11, all performance profiles of the intensified design remain in the red polygons, so the intensified design passes the design validation and further iterations are not necessary. In contrast, none of the deterministic designs passes the validation process. As the randomly generated feedstock compositions contain a moderate amount of acid gases and NGLs relative to the compositions of Feeds #1–#8, additional separation is required. The deterministic designs #1–#4 are suitable for dry gas with more acid gases, but they are insufficient in separating NGLs, resulting in high

— 1B — 2B — 3B — 4B — 5B — 6B — 7B — 8B — IB — Upper Bound

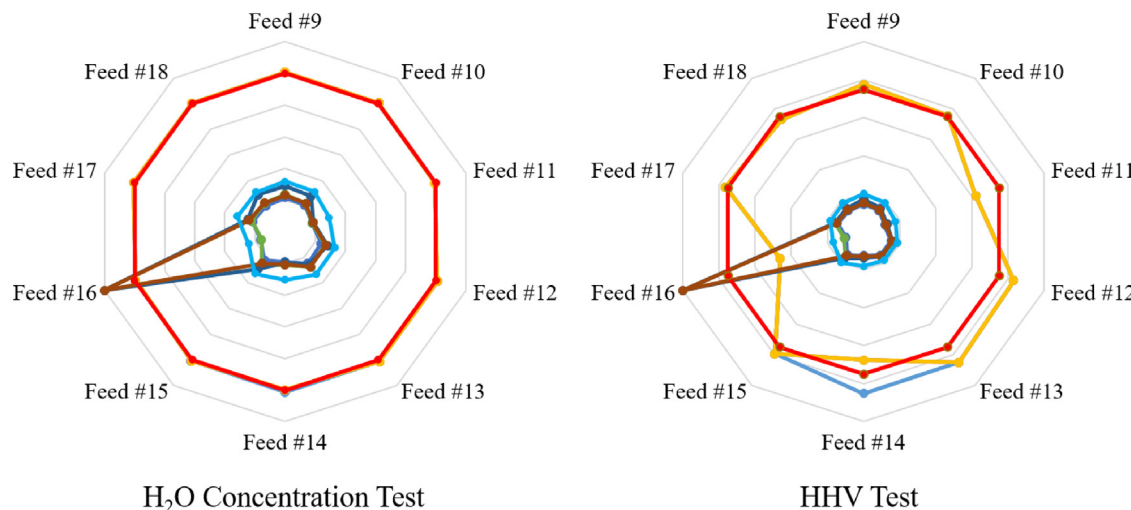


Fig. 11. H_2O concentration and higher heating value test results for the deterministic and intensified designs based on the proposed process system. Each performance profile is noted by two characters. The first character represents the type of designs: numbers denote the deterministic designs and “I” denotes the intensified designs. The second character is “B”, which denotes the proposed process system.

HHVs in the product gas. Deterministic designs #5–#8 excel in handling wet gas, but they are not good at effectively reducing the acid gas concentrations into a desired range. It is noted that the amount of acid gases in Feed #16 is beyond the separation capability of deterministic design #7 and #8, so we assign performance results to these infeasible designs to ensure the corresponding points are located outside the red polygons. Overall, the intensified design of the proposed system achieves thorough separation of all undesired components and NGLs simultaneously, and is effectively hedged against uncertain feedstock compositions.

It is noted that even though we test limited feedstock compositions, the wide composition coverage provides a high confidence of robustness in the obtained intensified design. Furthermore, the intensified design is more robust and cost-effective than any deterministic design. When the feedstock composition fluctuates, it is risky that a deterministic design is unable to completely process the raw shale gas. The resulting off-spec products will be rejected in downstream distribution networks. Consequently, the processing facility may have to purchase more expensive raw shale gas from other shale wellsites to adjust the feed composition, or it will have to shut down the entire process to prevent serious impact on the downstream systems. In contrast, the intensified design can operate continuously as long as the raw shale gas comes from the same wellsites. Therefore, it is worthwhile to consider and apply intensified design instead of deterministic designs.

6. Conclusion

In this work, we developed a systematic simulation-based process intensification method for handling uncertain feedstock compositions in shale gas processing and NGLs recovery process systems. The method included process simulation, capacity-oriented process intensification, and design validation, which communicated with each other in an iterative manner. The method was illustrated using a conventional process system and a novel process system, the latter of which considered an integrated condensation-based gas dehydration and turboexpander-based NGLs recovery process. In the techno-economic analysis, the intensified design of the novel system showed a lower unit annualized cost per 1 MMBTU of raw shale gas than that of the conventional

system. We conducted 4 groups of tests for the intensified and deterministic designs. We found that the intensified design of the novel system could effectively handle uncertain feedstock compositions.

Acknowledgement

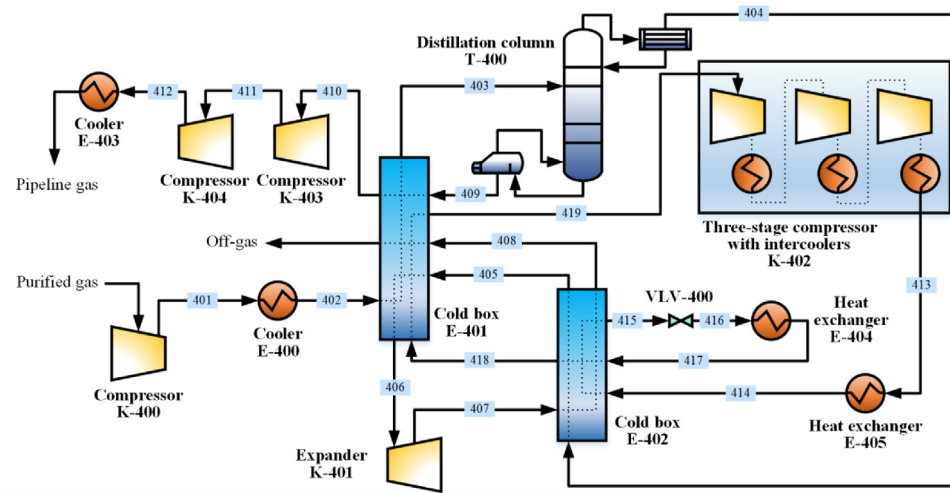
The authors acknowledge financial support from National Science Foundation (NSF) CAREER Award (CBET-1643244).

Appendix A. : Nitrogen Rejection Process

In case that nitrogen affects the quality of pipeline gas, a nitrogen rejection section can be added after the NGLs recovery section as shown in Fig. A1. In stead of being treated by heaters and compressors in the NGLs recovery process, stream 309 (the conventional process system) or stream 214 (the proposed process system) is pressurized to 30 bar by K-400 and cooled to -105°C by E-400 before being fed to a distillation column T-400. The cooling energy in the condenser of T-400 is provided by E-404, while the heating energy in the reboiler of T-400 is provided by E-405. The gas from the overhead of T-400 contains nitrogen and methane at -135°C , and it is used as a cooling source in cold boxes E-401 and E-402. The extra pressure head of Stream 406 is utilized for electricity generation via a turboexpander K-401. Consequently, the temperature of Stream 407 is reduced to -103.4°C , and the gas is used as a cooling source again in E-401 and E-402. Due to a large amount of methane contained in the off-gas, it is later sent to a combustor together with the other off-gas streams. The liquid from the bottom of T-400 is heated and pressurized so that they are qualified for distribution in pipeline systems. An internal cooling cycle (Streams 413–419) is embedded in the process. A low temperature of 142.4°C of Stream 416 is obtained as a result of a significant pressure drop at valve VLV-400, and the pressure is later elevated by a three-stage compression system K-402.

Appendix B. : Evaluation results of the conventional process system

See Tables B1–B4

**Fig. A1.** Process flowsheet of nitrogen rejection.**Table B1**

Mass balance results for the deterministic designs based on the conventional process system.

	Design #1	Design #2	Design #3	Design #4	Design #5	Design #6	Design #7	Design #8
Input								
Raw shale gas (MMSCDF)	191.82	189.75	189.47	191.08	222.68	226.06	242.14	219.67
Hydrogen (kg/h)	2.43	2.41	2.41	2.42	2.83	2.87	3.04	2.79
MEA (kg/h)	3.92	3.90	3.90	3.91	11.73	13.13	16.79	11.95
MDEA (kg/h)	0.48	0.40	0.39	0.44	0.21	0.23	0.26	0.21
TEG (kg/h)	0.32	0.32	0.32	0.32	1.55	1.83	2.55	1.60
Process water (tonne/h)	0.82	0.66	0.92	0.78	0.49	0.52	0.63	0.53
Output								
Pipeline gas (MMSCDF)	181.56	181.53	181.53	181.76	179.90	179.58	178.88	179.99
NGLs (tonne/h)	0.00	0.00	0.00	0.00	78.07	83.08	118.73	70.50
Sulfur (tonne/h)	0.69	0.69	0.69	0.69	0.81	0.82	0.87	0.79
Direct emissions								
CO ₂ (tonne/h)	20.94	16.51	15.97	18.90	3.67	4.33	6.02	3.90
SO ₂ (kg/h)	6.30	7.65	7.41	8.68	1.89	1.87	2.40	1.89
H ₂ S (kg/h)	8.40	4.62	4.38	6.43	10.24	13.05	23.15	11.26

Table B2

Energy balance results for the deterministic designs based on the conventional process system.

	Design #1	Design #2	Design #3	Design #4	Design #5	Design #6	Design #7	Design #8
Feed ($\times 10^3$ MMBTU/h)								
Raw shale gas	7.63	7.62	7.62	7.63	11.39	11.64	13.34	11.03
Utility (GJ/h or specified)								
Electricity (MW)	3.74	3.63	3.61	3.70	8.13	8.12	8.19	8.10
Cooling Water	134.94	132.72	132.39	134.08	71.34	71.09	75.36	67.58
Refrigerant 1	0.00	0.00	0.00	0.00	41.43	40.82	47.45	41.50
LP Steam Generation	2.73	2.56	2.53	2.65	2.03	2.07	2.25	2.00
HP Steam Generation	5.11	4.93	4.89	5.03	4.86	4.94	5.29	4.80
LP Steam	0.00	0.00	0.00	0.00	18.95	14.67	11.76	17.55
MP Steam	310.00	296.07	294.78	304.40	49.59	59.15	67.34	51.10
HP Steam	0.75	0.75	0.75	0.75	4.79	5.11	5.60	4.82
Fired Heat	11.90	11.39	11.28	11.67	10.60	10.78	11.58	10.46
Product ($\times 10^3$ MMBTU/h or specified)								
Pipeline gas	7.62	7.62	7.62	7.62	7.62	7.62	7.62	7.62
NGLs	0.00	0.00	0.00	0.00	3.75	4.00	5.69	3.39
Sulfur (MMBTU/h)	6.01	5.97	5.96	5.99	7.00	7.09	7.51	6.89

Table B3

Economic evaluation results based on the conventional process system.

	Design #1	Design #2	Design #3	Design #4	Design #5	Design #6	Design #7	Design #8	Intensified Design
Total direct cost (MM\$)	15.32	14.92	14.90	15.21	38.28	34.01	80.34	25.41	83.70
Indirect cost (MM\$)	4.9	4.8	4.8	4.9	12.2	10.9	25.7	8.1	26.8
Feedstock cost (MM\$/year)	109.8	109.8	109.8	109.8	164.1	167.6	192.1	158.9	192.1
Utility cost (MM\$/year)	8.2	7.8	7.8	8.0	9.3	9.4	10.1	9.3	10.1
Total annualized cost (MM\$/year)	121.2	120.8	120.8	121.1	181.4	184.2	219.2	173.5	219.9
Unit annualized cost (\$/MMBTU)	1.99	1.98	1.98	1.98	1.99	1.98	2.05	1.97	2.06

Table B4

Operating operations of key operating units in the deterministic designs based on the conventional process system. In each cell, the first value represents the lower bound, and the second value represents the upper bound.

	Design #1	Design #2	Design #3	Design #4	Design #5	Design #6	Design #7	Design #8
T-100 P(bar)	42.0, 42.4	42.0, 42.4	42.0, 42.4	42.0, 42.4	42.0, 42.4	42.0, 42.4	42.0, 42.4	42.0, 42.4
T-100 T(°C)	37.3, 91.0	37.3, 96.3	37.4, 97.0	37.3, 92.8	37.8, 55.8	38.7, 59.6	40.3, 66.2	38.2, 58.3
T-101 P(bar)	1.9, 2.0	1.9, 2.0	1.9, 2.0	1.9, 2.0	1.9, 2.0	1.9, 2.0	1.9, 2.0	1.9, 2.0
T-101 T(°C)	112.6, 122.3	113.8, 122.4	113.9, 122.4	113.2, 122.3	99.1, 121.7	106.5, 121.9	103.1, 121.9	100.2, 121.7
T-102 P(bar)	0.6, 0.7	0.6, 0.7	0.6, 0.7	0.6, 0.7	0.6, 0.7	0.6, 0.7	0.6, 0.7	0.6, 0.7
T-102 T(°C)	30.4, 34.4	30.3, 33.8	30.3, 33.8	30.3, 34.1	30.2, 36.1	30.2, 36.5	30.4, 37.2	30.3, 36.3
T-103 P(bar)	1.5, 1.6	1.5, 1.6	1.5, 1.6	1.5, 1.6	1.5, 1.6	1.5, 1.6	1.5, 1.6	1.5, 1.6
T-103 T(°C)	58.0, 117.2	58.9, 117.2	59.3, 117.2	58.3, 117.2	62.3, 117.2	60.5, 117.2	59.7, 117.2	61.1, 117.2
T-104 P(bar)	1.0, 1.1	1.0, 1.1	1.0, 1.1	1.0, 1.1	1.0, 1.1	1.0, 1.1	1.0, 1.1	1.0, 1.1
T-104 T(°C)	30.1, 31.6	30.1, 31.4	30.1, 31.4	30.1, 31.5	30.1, 32.3	30.1, 32.4	30.1, 32.6	30.1, 32.3
T-200 P(bar)	41.5, 42.0	41.5, 42.0	41.5, 42.0	41.5, 42.0	41.5, 42.0	41.5, 42.0	41.5, 42.0	41.5, 42.0
T-200 T(°C)	38.0, 38.5	38.0, 38.6	38.0, 38.6	38.0, 38.5	49.0, 49.9	50.6, 51.6	52.2, 53.2	49.9, 50.9
T-201 P(bar)	1.0, 1.1	1.0, 1.1	1.0, 1.1	1.0, 1.1	1.0, 1.1	1.0, 1.1	1.0, 1.1	1.0, 1.1
T-201 T(°C)	97.9, 195.0	97.9, 195.0	97.9, 195.0	97.9, 195.0	87.6, 200.0	88.4, 200.0	89.0, 200.0	88.1, 200.0
T-202 P(bar)	1.1, 1.2	1.1, 1.2	1.1, 1.2	1.1, 1.2	1.1, 1.2	1.1, 1.2	1.1, 1.2	1.1, 1.2
T-202 T(°C)	183.5, 190.5	183.4, 190.4	183.5, 190.5	183.4, 190.4	186.2, 194.5	186.4, 194.6	185.9, 194.6	186.3, 194.5
T-300 P(bar)	N/A	N/A	N/A	N/A	22.5, 23.0	22.5, 23.0	22.5, 23.0	22.5, 23.0
T-300 T(°C)	N/A	N/A	N/A	N/A	-96.3, 20.5	-95.3, 19.0	-91.9, 24.5	-96.4, 19.0

References

- Allen, D.T., Torres, V.M., Thomas, J., Sullivan, D.W., Harrison, M., Hendler, A., et al., 2013. Measurements of methane emissions at natural gas production sites in the United States. *Proc. Natl. Acad. Sci. U. S. A.* 110, 17768–17773.
- AspenTech, 2010a. *Aspen HYSYS Customization Guide*. Aspen Technology, Inc., Burlington, MA, USA.
- AspenTech, 2010b. *Aspen Energy Analyzer User Guide*. Aspen Technology, Inc., Burlington, MA, USA.
- AspenTech, 2010c. *Aspen Process Economic Analyzer V7.2 User Guide*. Aspen Technology, Inc., Burlington, MA, USA.
- Bullin, K.A., Krouskop, P.E., 2009. Compositional variety complicates processing plans for US shale gas. *Oil Gas J.* 107, 50–55.
- EIA, (2006, September 2015). Natural Gas Processing: The Crucial Link Between Natural Gas Production and Its Transportation to Market. Available: http://www.eia.gov/pub/oil_gas/natural_gas/feature_articles/2006/ngprocess/ngprocess.pdf.
- EIA, 2015. *Annual Energy Outlook*, Washington DC DOE/EIA-0383(2015), pp. 2015.
- Ehlinger, V.M., Gabriel, K.J., Noureldin, M.M.B., El-Hawagi, M.M., 2014. Process design and integration of shale gas to methanol. *ACS Sustain. Chem. Eng.* 2, 30–37.
- energytransfer.com. (2012, May, 2016). Y-grade product specifications. Available: <http://www.energytransfer.com/documents/UniformY-Grade%20Specs-LSTV111612.pdf>.
- Errico, M., Rong, B.-G., Tola, G., Turunen, I., 2008. Process intensification for the retrofit of a multicomponent distillation plant an industrial case study. *Ind. Eng. Chem. Res.* 47, 1975–1980.
- Esteban, A., Hernandez, V., Lunsford, K., 2000. Exploit the benefits of methanol. In: *79th GPA Annual Convention*, Atlanta, GA, USA.
- F. Power (2016, May, 2016). FGE EAGLE PINES. Available: <http://fgepower.com/eagle-pines/>.
- Fout, T., Zoelle, A., Keairns, D., Turner, M., Woods, M., Kuehn, N., et al., 2015. *Cost and Performance Baseline for Fossil Energy Plants Volume 1a: Bituminous Coal (PC) and Natural Gas to Electricity Version 3*, South Park Township PA DOE/NETL-2015/1723.
- Freeman, C., Moridis, G.J., Michael, G.E., Blasingame, T.A., 2012. Measurement, modeling, and diagnostics of flowing gas composition changes in shale gas wells. *SPE Latin America and Caribbean Petroleum Engineering Conference*.
- Freund, H., Sundmacher, K., 2008. Towards a methodology for the systematic analysis and design of efficient chemical processes: part 1. From unit operations to elementary process functions. *Chem. Eng. Process. Process Intensif.* 47, 2051–2060.
- GPSA, 2012. *Engineering Data Book*, 13 ed. Gas Processors Suppliers Association, Tulsa, Oklahoma, USA.
- Gao, J., You, F., 2015a. Shale gas supply chain design and operations toward better economic and life cycle environmental performance: MINLP model and global optimization algorithm. *ACS Sustain. Chem. Eng.* 3, 1282–1291.
- Gao, J., You, F., 2015b. Deciphering and handling uncertainty in shale gas supply chain design and optimization: novel modeling framework and computationally efficient solution algorithm. *AIChE J.* 61, 3739–3755.
- Gao, J., You, F., 2015c. Optimal design and operations of supply chain networks for water management in shale gas production: MILFP model and algorithms for the water-energy nexus. *AIChE J.* 61, 1184–1208.
- Getu, M., Mahadzir, S., Long, N.V.D., Lee, M., 2013. Techno-economic analysis of potential natural gas liquid (NGL) recovery processes under variations of feed compositions. *Chem. Eng. Res. Des.* 91, 1272–1283.
- Goellner, J.F., 2012. Expanding the shale gas infrastructure. *Chem. Eng. Prog.* 49–59.
- Gong, J., You, F., 2015. Sustainable design and synthesis of energy systems. *Curr. Opin. Chem. Eng.* 10, 77–86.
- Gong, J., You, F., 2016. Optimal processing network design under uncertainty for producing fuels and value-added bioproducts from microalgae: two-stage adaptive robust mixed integer fractional programming model and computationally efficient solution algorithm. *AIChE J.*, <http://dx.doi.org/10.1002/aiic.15370>.
- Gong, J., Garcia, D.J., You, F., 2016. Unraveling optimal biomass processing routes from bioconversion product and process networks under uncertainty: an adaptive robust optimization approach. *ACS Sustain. Chem. Eng.* 4, 3160–3173.
- He, C., You, F., 2014. Shale gas processing integrated with ethylene production: novel process designs, exergy analysis, and techno-economic analysis. *Ind. Eng. Chem. Res.* 53, 11442–11459.
- He, C., You, F., 2015. Toward more cost-effective and greener chemicals production from shale gas by integrating with bioethanol dehydration: novel process design and simulation-based optimization. *AIChE J.* 61, 1209–1232.
- He, C., You, F., 2016. Deciphering the true life cycle environmental impacts and costs of the mega-scale shale gas-to-olefins projects in the United States. *Energy Environ. Sci.* 9, 820–840.
- Johnson, K., 2009. Natural gas processors respond to rapid growth in shale gas production. *Am. Oil Gas Rep.*
- Julian-Duran, L.M., Ortiz-Espinoza, A.P., El-Halwagi, M.M., Jimenez-Gutierrez, A., 2014. Techno-economic assessment and environmental impact of shale gas alternatives to methanol. *ACS Sustain. Chem. Eng.* 2, 2338–2344.
- Kerr, R.A., 2010. Natural gas from shale bursts onto the scene. *Science* 328, 1624–1626.
- Kidnay, J., Parrish, W.R., McCartney, D.G., 2011a. Overview of gas plant processing. In: *Fundamentals of Natural Gas Processing*, second ed. CRC Press, pp. 149–160.
- Kidnay, J., Parrish, W.R., McCartney, D.G., 2011b. Gas treating. In: *Fundamentals of Natural Gas Processing*, second edition. CRC Press, pp. 211–241.
- Lira-Barragan, L.F., Ponce-Ortega, J.M., Guillen-Gosálbez, G., El-Halwagi, M.M., 2016. Optimal water management under uncertainty for shale gas production. *Ind. Eng. Chem. Res.* 55, 1322–1335.
- Liu, P., Georgiadis, M.C., Pistikopoulos, E.N., 2011. Advances in energy systems engineering. *Ind. Eng. Chem. Res.* 50, 4915–4926.
- Lozowski, D., 2015. Economic indicators. *Chem. Eng.* 122, 96.
- Lutze, P., Gani, R., Woodley, J.M., 2010. Process intensification: a perspective on process synthesis. *Chem. Eng. Process.* 49, 547–558.
- Lutze, P., Román-Martínez, A., Woodley, J.M., Gani, R., 2012. A systematic synthesis and design methodology to achieve process intensification in (bio) chemical processes. *Comput. Chem. Eng.* 36, 189–207.
- Lutze, P., Babi, D.K., Woodley, J.M., Gani, R., 2013. Phenomena based methodology for process synthesis incorporating process intensification. *Ind. Eng. Chem. Res.* 52, 7127–7144.
- Minkkinen, A., Rojey, A., Charron, Y., Lebas, E., 1998. Technological developments in sour gas processing. In: Rojey, A. (Ed.), *Gas Cycling: A New Approach*. Editions Technip, Paris.
- Mokhatab, S., Poe, W.A., Speight, J.G., 2006. *Handbook of Natural Gas Transmission and Processing*. Gulf Publishing Company, Burlington, MA, USA.
- Moulijn, J.A., Stankiewicz, A., Grievink, J., Góral, A., 2008. Process intensification and process systems engineering: a friendly symbiosis. *Comput. Chem. Eng.* 32, 3–11.
- Netusil, M., Dittl, P., 2011. Comparison of three methods for natural gas dehydration. *J. Nat. Gas. Chem.* 20, 471–476.
- Ponce-Ortega, J.M., Al-Thubaiti, M.M., El-Halwagi, M.M., 2012. Process intensification: new understanding and systematic approach. *Chem. Eng. Process.* 53, 63–75.
- Pring, M., 2012. Condensate Tank Oil and Gas Activities. Eastern Research Group, Inc., Austin, TX, USA.

- Reed, M., 2013. Shale plays should see added capacity next 2 years. *Pipeline Gas J.* 240.
- Rufford, T.E., Smart, S., Watson, G.C.Y., Graham, B.F., Boxall, J., Diniz da Costa, J.C., et al., 2012. The removal of CO₂ and N₂ from natural gas: a review of conventional and emerging process technologies. *J. Petrol. Sci. Eng.* 95, 123–154.
- Salkuyeh, Y.K., Adams, T.A., 2015. A novel polygeneration process to co-produce ethylene and electricity from shale gas with zero CO₂ emissions via methane oxidative coupling. *Energy Convers. Manage.* 92, 406–420.
- Shi, H., You, F., 2016. A computational framework and solution algorithms for two-stage adaptive robust scheduling of batch manufacturing processes under uncertainty. *AIChE J.* 62, 687–703.
- Siiroila, J.J., 2014. The impact of shale gas in the chemical industry. *AIChE J.* 60, 810–819.
- Speight, J.G., 2013. Chapter 4 – shale gas properties and processing. In: Speight, J.G. (Ed.), *Shale Gas Production Processes*. Gulf Professional Publishing, Boston, pp. 101–119.
- Wang, M.Q., Xu, Q., 2014. Optimal design and operation for simultaneous shale gas NGL recovery and LNG re-gasification under uncertainties. *Chem. Eng. Sci.* 112, 130–142.
- Yang, L.L., Grossmann, I.E., Manno, J., 2014. Optimization models for shale gas water management. *AIChE J.* 60, 3490–3501.
- Yue, D., You, F., 2016. Optimal supply chain design and operations under multi-scale uncertainties: nested stochastic robust optimization modeling framework and solution algorithm. *AIChE J.* 62, 3041–3055.
- Zavala-Araiza, D., Allen, D.T., Harrison, M., George, F.C., Jersey, G.R., 2015. Allocating methane emissions to natural gas and oil production from shale formations. *ACS Sustain. Chem. Eng.* 3, 492–498.